Journal of
Applied
Crystallography
ISSN 0021-8898

Received 16 August 2006
Accepted 9 November 2006

Investigation of symmetry-breaking flux-line lattice phases in superconductors by small-angle neutron scattering

Edward Forgan,[a]* Mark Laver[a,b] and Charlotte Bowell[a]

[a]School of Physics and Astronomy, University of Birmingham, Birmingham B15 2TT, United Kingdom, and [b]Institut Laue-Langevin, F-38042, Grenoble, France. Correspondence e-mail: e.m.forgan@bham.ac.uk

In single-crystal superconductors in the mixed state, flux-line structures may have a lower symmetry than the host crystal. In this case, multiple degenerate flux lattice domains may be present simultaneously and give rise to complicated small-angle diffraction patterns. The interpretation of these patterns in terms of the flux lattice structure in a single domain is discussed, with particular reference to recently reported spontaneous symmetry-breaking flux-line lattice phases in niobium.

1. Introduction

When a sufficiently large magnetic field is applied to a type II superconductor, the field enters the superconductor in the form of quantized flux lines, each surrounded by a vortex of super-current, and each carrying one quantum of magnetic flux, $\Phi_0 = h/2e$. In the absence of pinning, these lines arrange themselves in the form of a two-dimensional flux-line lattice. In the simplest possible isotropic case, the flux lattice has a regular hexagonal structure, and all orientations of this flux lattice relative to the underlying crystal lattice of the superconductor have the same energy. In practice in real crystals, the flux lattice structure may well be in a distorted or non-hexagonal coordination and is generally aligned with its basis vectors in a definite relationship to those of the crystal. The cause of this alignment is as follows: to lowest order there is degeneracy with respect to flux lattice orientation; thus, *any* additional interaction, however small, will be able to cause alignment. This may be due to intrinsic causes, such as crystalline anisotropy, or extrinsic ones, such as pinning by twin planes in high-T_c superconductors, or alignment with the external faces of a crystal. Furthermore, it is known that in the isotropic case the hexagonal and square flux lattice structures only differ in free energy by a few percent, so that quite weak sources of anisotropy may lead to a severe distortion of the flux lattice structure away from undistorted simple hexagonal structure. However, unless the flux lattice has the same symmetry about the field axis as the underlying crystal, there will be several flux lattice domain orientations with identical energies. If randomly nucleated, these different domains will be present in approximately equal proportions, and a resulting small-angle neutron scattering (SANS) diffraction pattern will be a superposition of the patterns due to the individual domains. This paper is about simple techniques to interpret these patterns in terms of the contributions of individual flux lattice domain orientations. Once the flux lattice structure of one domain is known, we may attempt to interpret its structure and distortion in terms of anisotropy of Fermi surface, or of the superconducting energy gap, or in terms of extrinsic effects.

2. Methods of interpretation of flux lattice diffraction patterns

For achievable fields and neutron wavelengths, the flux lattice spacing is much larger than the neutron wavelength so scattering angles are small and SANS is the appropriate technique. In the usual (but not the only possible) SANS geometry for investigating a flux-line lattice (FLL), the magnetic field is approximately parallel to the incoming neutron beam. If the sample and field are rocked together by small angles about a horizontal or vertical axis perpendicular to the neutron beam, various FLL Bragg planes will be brought into the diffracting condition and each will give rise to a diffraction spot on a two-dimensional multi-detector. A sum of the intensities over all rocking angles will give a diffraction pattern that is an image of the (planar) reciprocal lattice of the FLL, and all diffraction spots will appear at positions given by (sums of) the reciprocal lattice vectors of any particular FLL domain present in the sample. Because of its two-dimensional nature, the real-space FLL has exactly the same shape as the reciprocal lattice, but rotated by 90° about the field axis, and scaled. In Fig. 1 are shown schematic diffraction patterns (*a*) from a single square FLL which is aligned with the crystal axes, typically seen in a high-T_c superconductor at high fields (*e.g.* Brown *et al.*, 2004); (*b*) from a pair of FLL domains, such as would be obtained in niobium at low fields and high temperatures (Laver *et al.*, 2006), and (*c*) from a single domain contributing to the pattern in (*b*). It will be noted that the total diffraction pattern in case (*b*) has the same symmetry about the field axis as the crystal, even though the individual FLL domains giving rise to it do not.

2.1. Removal of degeneracy

The simplest technique to isolate individual flux lattice domains is to remove the degeneracy between them by rotating the sample relative to the field, so that the different domains are distinct in energy. In a typical neutron scattering cryostat, rotation of the sample stick about a vertical axis is easily performed. In the case shown in Fig. 1(*b*), a rotation of ~5° is sufficient to completely remove half the spots when the flux lattice is reformed by cooling through T_c, and the resulting pattern is shown in Fig. 1(*c*). It represents a distorted hexagonal lattice, with the half unit cell an isosceles triangle whose base is approximately equal to its height. The base is parallel to a <100> direction in niobium. It is clear that the symmetry-related domain with the FLL rotated by 90° about the field axis will be degenerate if the field is exactly along [001], and that equally populated domains will give the symmetrical pattern shown in Fig. 1(*b*).

In Fig. 2(*a*) is shown experimental data obtained in niobium cooled to 2 K with a field of 0.16 T applied along the [001] direction [a lower temperature than the case represented in Fig. 1(*b*)]. In these results, the crystal <100> axes were oriented at ~9° to the horizontal and vertical directions in the figure. Rotation by 5° about the vertical axis was sufficient to remove some of the FLL domains, but the spots away from the crystal axes were still double. It required a rotation of 15° to remove sufficiently the remaining degeneracy and give the almost single-domain pattern seen in Fig. 2(*c*). (Note that the misalignment of the crystal axes by 9° relative to the vertical rotation axis was necessary to permit the rotation to remove the remaining degeneracy.) We now see clearly that the basic FLL domain has a half unit cell that is scalene-triangular, *i.e.* the lowest possible symmetry 2*d* Bravais lattice, despite the fact that it is formed within an underlying crystal possessing fourfold rotation symmetry and two mirror planes. It should be noted that there is no symmetry requirement for one pair of the diffraction spots to lie along a <100> direction, although this is the case within experimental resolution. However, at higher fields, we have sufficient resolution to observe that these spots move steadily away from the symmetry directions (see Laver *et al.*, 2006). It is quite remarkable that the FLL structure spontaneously and so comprehensively breaks the underlying crystal symmetry, although once again we observe that the total diffraction pattern from all four FLL domains has the square symmetry of the underlying crystal. It is therefore important to disentangle the domain effects to be certain of the FLL symmetry.

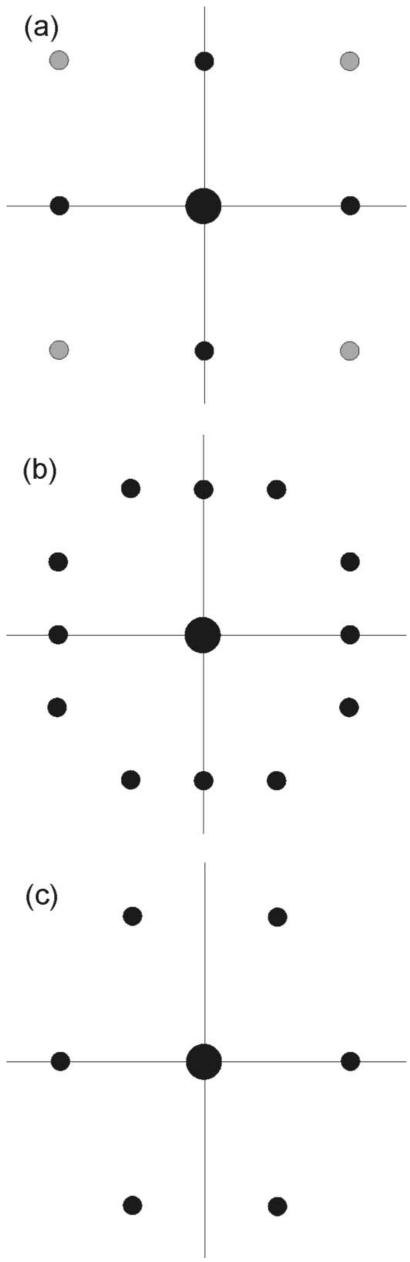

Figure 1
Schematic diffraction patterns: (*a*) for a single-domain square FLL, with first and second order spots; (*b*) for a two-domain distorted hexagonal FLL (first order spots only); (*c*) for one of the domains contributing to (*b*). The central spot represents the main neutron beam. In (*a*) the horizontal and vertical lines would lie along the <110> directions for the high-T_c material $YBa_2Cu_3O_7$ at high fields. In (*b*) these lines lie along the [100] and [010] directions for niobium with the magnetic field applied along the fourfold [001] direction.

One final remark may be appropriate here: random domain nucleation or slight experimental misalignments may cause different volume fractions of otherwise equivalent domains. It may therefore be possible by careful measurements of integrated intensities to associate certain diffraction spots together and to deduce the structure of a single domain without the need for sample rotation. This approach may be combined with those described in the following sections.

2.2. Use of Bravais lattice properties

Except at very low fields in layered superconductors (where direct imaging reveals complicated and sometimes disordered structures), all FLLs observed so far form simple Bravais lattices, with only one vortex per unit cell. Hence, the positions of all the diffraction spots from a single FLL domain may be expressed as linear combinations of two basis vectors of the FLL reciprocal lattice with no systematic absences. This fact may be used to select spots belonging to a single domain, from a diffraction pattern containing contributions from several domains. Consider the spots labelled by their reciprocal lattice vectors $\mathbf{q}_1$ and $\mathbf{q}_2$ in Fig. 3. If they belong to the same FLL domain, then there should also be a diffraction spot at $\mathbf{q}_3 = \mathbf{q}_2 - \mathbf{q}_1$. The absence of such a spot indicates that $\mathbf{q}_1$ and $\mathbf{q}_2$ do not belong to the same domain. However, $\mathbf{q}_3$ and $\mathbf{q}_4$ imply the existence of $\mathbf{q}_5$, which does exist, and belongs to the same domain. In this way, the picture of Fig. 1(*c*) may be confirmed. Similar techniques may be used to confirm the identification of the FLL domains contributing to the diffraction patterns in Fig. 2. A confirmation of the chosen domain structures is given by the observation that the two FLL structures contributing to Fig. 1(*c*) [or the four to Fig. 2(*a*)] have exactly the same shape as each other and the same relationship to the underlying crystal structure. This would be expected, since they are all present because they are degenerate with each other.

One minor caveat should be added here: with strong scatterers like niobium, multiple scattering between two different FLL domains can occur and give rise to spots that satisfy the conditions above. The four very weak spots in the corners of the square pattern in Fig. 2(*a*) are due to this cause.

2.3. Use of flux quantization

Any FLL structure with one flux line per unit cell will have its unit cell area A necessarily related to the average induction B by $A = \Phi_0/B$. In reciprocal space, this translates to an area $A_q = 4\pi^2 B/\Phi_0$, which is, for instance, the area contained within the parallelogram subtended by $\mathbf{q}_4$ and $\mathbf{q}_5$. Hence, by careful measurements of spot positions, the value of flux density implied by an FLL structure may be obtained. In many cases the value of the average

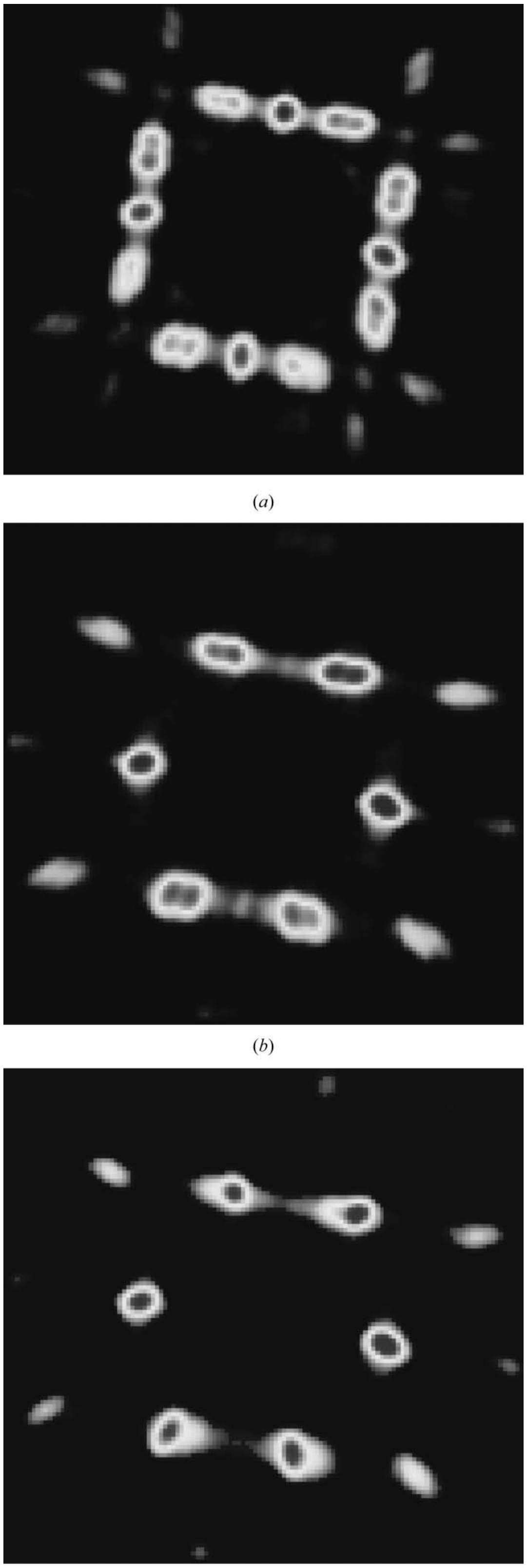

Figure 2
Diffraction patterns obtained from the FLL in niobium at low temperature (*a*) with the field along [001]; (*b*) with the crystal [001] direction rotated by 5° about the vertical axis away from the field direction; (*c*) with 15° rotation about the same axis. In (*a*) four FLL domains are present; in (*b*) two of them have been removed, and in (*c*) the dominant contributions are from a single FLL domain.

induction will be known. If the FLL is prepared by cooling in a field through T_c, then the induction will be closely equal to that applied, either if the field is well above H_{c1}, or if pinning is strong. In such a case, even the value of q may be sufficient to distinguish between a square and a hexagonal FLL in cases where the intensity is low and the domain arrangement is sufficiently disordered that it is difficult to identify individual spots [see for example Gilardi *et al.* (2004)]. In other cases, the average induction may be known from magnetization measurements, or alternatively, diffraction measurements may be used to derive the average induction in an FLL domain, and even show that not all the crystal is occupied by an FLL in the intermediate mixed state in niobium (Christen *et al.*, 1977; Laver *et al.*, 2006)

3. Theoretical considerations about FLL structures

Two simple theories of FLL structure, are the Ginzburg–Landau (GL) theory, originally used by Abrikosov to predict the existence of the flux lattice, and the London theory, in which the vortex cores are ignored [see, for example, Tinkham (1996), for an account of these theories]. GL theory is strictly valid only near the critical temperature T_c, but gives a qualitatively useful picture of the FLL at lower temperatures. London theory is simpler and is applicable at all temperatures, but is only reliable at inductions well below the upper critical field B_{c2} where the vortex cores overlap. In both these theories, the anisotropy of the superconducting electrons in a crystal is essentially that of the electron effective mass, which may be represented by a second-rank tensor. Within any crystal plane with four- or sixfold rotation symmetry, the effective mass is independent of angle, and in a cubic crystal such as niobium, the effective mass, like the resistivity, is completely isotropic. If the field is applied parallel to a principal axis in a lower symmetry, such as orthorhombic, these theories may be reduced to the isotropic case by a scale transformation (see *e.g.* Campbell *et al.*, 1988). Hence, under these circumstances, and at this level of explanation, no alignment of the FLL with the crystal axes is expected. Also, the FLL should have a regular hexagonal structure, only distorted by a scale transformation if appropriate. These considerations are likely to be particularly applicable at low inductions in strongly type-II superconductors, in

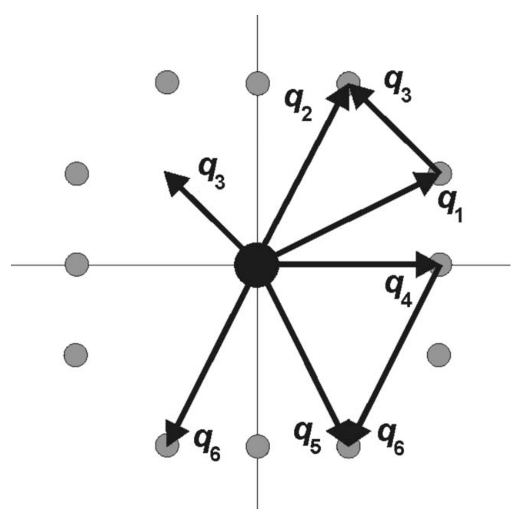

Figure 3
The two-domain schematic diffraction pattern of Fig. 1(*b*), used to demonstrate how the Bravais property of the FLL may be used to select which spots belong to which domain (for details see text).

which the flux-lines cores are well separated; in such cases, the external faces of a crystal may be the cause of the FLL alignment.

3.1. Effects of Fermi surface and gap anisotropy

Extensions have been proposed to the GL theory (De Wilde *et al.*, 1997) and London theory (Kogan *et al.*, 1997) that allow the interaction between the spatial variation of the superconducting order parameter and the Fermi surface anisotropy to be taken into account. Of equal importance is the anisotropy of the superconducting energy gap, particularly in *d*-wave superconductors having nodes in the gap (see, for example Berlinsky *et al.*, 1995; Shiraishi *et al.*, 1999) and first-principles calculations have been performed of these effects combined (Nakai *et al.*, 2002). Essentially, the finite size and shape of the Cooper pairs are included, which allows the anisotropy of a 4th-rank tensor to appear. This can naturally give rise to distorted-triangular or square FLLs, such as those represented in Figs. 1(*a*) and 1(*c*), and also observed in the tetragonal borocarbide superconductors (see *e.g.* Kogan *et al.*, 1997; Paul *et al.*, 1998). However, it should be noted that all the FLL structures predicted by such theories are aligned with the crystal axes, unlike the FLLs with scalene-triangular coordination that give rise to the patterns in Fig. 2. Just as intriguing are square FLLs observed in niobium with the field along a fourfold direction (Laver *et al.*, 2006) which are *not* aligned with the crystal axes. These FLL structures therefore break the mirror symmetry of the crystal while retaining the rotational symmetry. A qualitative understanding of this may be obtained by assuming that there exists an interaction between flux lines that contains terms varying both as $\cos(4\phi)$ and $\cos(8\phi)$, where ϕ is the angle about the fourfold axis. Both these terms satisfy crystal symmetry, but their sum may have extrema at non-symmetry-determined values of ϕ. It may be that considerations such as this can give an account of both the rotated-square and scalene-triangular FLLs, but even so, the task remains to relate such qualitative ideas to the underlying Fermi surface and superconducting energy gap anisotropy, which are presumably the cause of these effects.

4. Summary and conclusions

Flux lattice structures can be reliably extracted from small-angle diffraction patterns, even when multiple FLL domains are present. The structures in pure crystals can tell us about the nature of the underlying superconducting state and the interactions between flux lines. Recent results obtained in niobium with the field parallel to a fourfold axis (Laver *et al.*, 2006) reveal flux lattice structures that spontaneously and comprehensively break the crystal symmetry and present challenges for our understanding of the superconductivity in this supposedly ‘conventional’ superconductor.

The important contributions to this work of S. P. Brown, D. Charalambous, R. J. Lycett, S. Ramos, D. Fort, R. Cubitt, C. D. Dewhurst and J. Kohlbrecher are gratefully acknowledged. Neutron scattering measurements referred to in this paper were performed on the SANS instruments at the Paul Scherrer Institut, Villigen, Switzerland, and the Institut Laue-Langevin, Grenoble France.

References

Berlinsky, A. J., Fetter, A. L., Franz, M., Kallin, C. & Soininen, P. I. (1995). *Phys. Rev. Lett.* **75**, 2200–2203.

Brown, S. P., Charalambous, D., Jones, E. C., Forgan, E. M., Kealey, P. G., Erb, A. & Kohlbrecher, J. (2004). *Phys. Rev. Lett.* **92**, 067004(4).

Campbell, L. J., Doria, M. M. & Kogan V. G. (1988). *Phys. Rev. B*, **38**, 2439–2443.

Christen, D. K., Tasset, F., Spooner, S. & Mook, H. A. (1977). *Phys. Rev. B*, **15**, 4506–4509.

De Wilde, Y., Iavarone, M., Welp, U., Metlushko, V., Koshelev, A. E., Aranson, I., Crabtree, G. W. & Canfield, P. C. (1997). *Phys. Rev. Lett.* **78**, 4273–4276.

Gilardi, R., Mesot, J., Brown, S. P., Forgan, E. M., Drew, A., Lee, S. L., Cubitt, R., Dewhurst, C. D., Uefuji, T. & Yamada, K. (2004). *Phys. Rev. Lett.* **93**, 217001(4).

Kogan, V. G., Bullock, M., Harmon, B., Miranovic, M., Dobrosavljevic Grujic, L., Gammel, P. L. & Bishop, D. J. (1997). *Phys. Rev. B*, **55**, R8693-R8696.

Laver, M., Forgan, E. M., Brown, S. P., Charalambous, D., Fort, D., Bowell, C., Ramos, S., Lycett, R. J., Christen, D. K., Kohlbrecher, J., Dewhurst, C. D. & Cubitt, R. (2006). *Phys. Rev. Lett.* **96**, 167002 (4).

Nakai, N., Miranović, P., Ichioka, M. & Machida, K. (2002). *Phys. Rev. Lett.* **89**, 237004 (4).

Paul, D. M. K., Tomy, C. V., Aegerter, C. M., Cubitt, R., Lloyd, S. H., Forgan, E. M., Lee, S. L. & Yethiraj, M. (1998). *Phys. Rev. Lett.* **80**, 1517–1520.

Shiraishi, J., Kohmoto, M. & Maki, K. (1999). *Phys. Rev. B*, **59**, 4497–4503.

Tinkham, M. (1996). *Introduction to superconductivity*, 2nd ed. New York: McGraw Hill.